A Linkage Map of an F₂ Hybrid Population of *Antirrhinum majus* and *A. molle*

Zsuzsanna Schwarz-Sommer,[*,1] Eugenia de Andrade Silva,[*] Rita Berndtgen,[*]
Wolf-Ekkehard Lönnig,[*] Andreas Müller,[*] Ingo Nindl,[*] Kurt Stüber,[*]
Jörg Wunder,[*] Heinz Saedler,[*] Thomas Gübitz,[†] Amanda Borking,[†]
John F. Golz,[†] Enrique Ritter[‡,1] and Andrew Hudson[†,1,2]

**Max Planck Institut für Züchtungsforschung, Carl-von-Linné-Weg 10, 50829 Köln, Germany, †Institute of Cell and Molecular Biology,
University of Edinburgh, Edinburgh EH9 3JH, United Kingdom and ‡Neiker, 01080 Vitoria, Spain*

ABSTRACT

To increase the utility of Antirrhinum for genetic and evolutionary studies, we constructed a molecular linkage map for an interspecific hybrid *A. majus* × *A. molle*. An F₂ population ($n = 92$) was genotyped at a minimum of 243 individual loci. Although distorted transmission ratios were observed at marker loci throughout the genome, a mapping strategy based on a fixed framework of codominant markers allowed the loci to be placed into eight robust linkage groups consistent with the haploid chromosome number of Antirrhinum. The mapped loci included 164 protein-coding genes and a similar number of unknown sequences mapped as AFLP, RFLP, ISTR, and ISSR markers. Inclusion of sequences from mutant loci allowed provisional alignment of classical and molecular linkage groups. The total map length was 613 cM with an average interval of 2.5 cM, but most of the loci were aggregated into clusters reducing the effective distance between markers. Potential causes of transmission ratio distortion and its effects on map construction were investigated. This first molecular linkage map for Antirrhinum should facilitate further mapping of mutations, major QTL, and other coding sequences in this model genus.

THE genus Antirrhinum (Plantaginacae or Veronicacae; OLMSTEAD *et al.* 2001) consists of ∼20 species that are native to the western Mediterranean region and mostly endemic to the Iberian Peninsula (SUTTON 1988). The species vary considerably in morphology, size, and habitat and include both small shrubs and herbs. All behave genetically as diploids, share the chromosome number of $2n = 16$, and form fertile hybrids when artificially cross-pollinated (RIEGER 1957; STUBBE 1966; W.-E. LÖNNIG, unpublished results). The genus also includes *Antirrhinum majus*, which has been domesticated as an ornamental over two millennia and adopted as a genetic model. Cultivated varieties and wild progenitors of *A. majus* and *A. siculum* are able to self-pollinate whereas all other members of the genus show gametophytic self-incompatibility and therefore are largely, or entirely, outbreeding. Self-incompatibility is determined by a single *S* locus in Antirrhinum and involves rejection of pollen grains carrying an *S* allele that is also present in the female (GRUBER 1932; EAST 1940; HERRMANN 1973).

Genetic variation within *A. majus* and between *A. majus* and other Antirrhinum species was first exploited in studies of inheritance in the mid-1800s (GODRON 1863;

DARWIN 1868). Following the later work of BAUR (1907) and WHELDALE (1907), *A. majus* was adopted more widely (reviewed by STUBBE 1966), resulting in a large collection of *A. majus* mutants, >400 of which survive (HAMMER *et al.* 1990). Genetically unstable mutations in loci required for anthocyanin pigmentation allowed isolation of three families of mutagenic transposons (BONAS *et al.* 1984; SOMMER *et al.* 1985; LUO *et al.* 1991). Because members of two families transpose by cut-and-paste mechanisms, they have been used as tags to clone genes or to generate mutations in sequences of unknown function. Over 40 genes and corresponding mutations have been identified in this way, including genes involved in floral meristem and organ identity (*e.g.*, COEN *et al.* 1990; SOMMER *et al.* 1990), asymmetry of flowers and lateral organs (*e.g.*, LUO *et al.* 1996; WAITES *et al.* 1998), cellular morphology (NODA *et al.* 1994), and pigmentation (*e.g.*, MARTIN *et al.* 1985; GOODRICH *et al.* 1992). Where tested, the majority of classical mutations have been caused by transposons that have subsequently become stable (*e.g.*, SOMMER *et al.* 1990; KUNZE *et al.* 1997). Antirrhinum is a member of the Asterid clade, which, together with the Rosids, comprise ∼75% of extant eudicots (SOLTIS *et al.* 1999). The more widely used model plant, *Arabidopsis thaliana*, is a Rosid and therefore parallel analysis in the two species has allowed identification of both conserved and divergent gene functions within dicots (*e.g.*, DAVIES *et al.* 1999).

A classical genetic map for *A. majus*, produced from mutant crosses, was composed of 57 morphological

---

[1]These authors contributed equally to this work.

[2]*Corresponding author:* Institute of Cell and Molecular Biology, University of Edinburgh, King's Bldgs., Mayfield Rd., Edinburgh EH9 3JH, UK. E-mail: andrew.hudson@ed.ac.uk

markers in eight linkage groups (LGs) and a total length of ~420 cM (Stubbe 1966). Cytologically visible deletions that unmasked recessive mutations allowed two linkage groups to be assigned tentatively to chromosomes distinguishable by size and by morphological features (Pohlendt 1942). Linkage analyses in crosses between *A. majus* mutants and several other species, including *A. molle,* revealed conservation of gene order within a substantial part of two chromosomes (Stubbe 1966), but estimates of map distances differed according to the species used as parents (Kühl 1937; Hoffmann 1949).

A molecular linkage map would allow full use of *A. majus* for comparative developmental studies and exploitation of the wide phenotypic variation within the genus Antirrhinum for genetic analysis of adaptation and species evolution. The primary aim of the work reported here was to construct a molecular linkage map for Antirrhinum using the F_2 progeny of an *A. majus* × *A. molle* hybrid. Distorted transmission ratios were detected at the majority of loci. Using available mapping software in a strategy that minimized the effects of distortion, markers at a minimum of 243 loci were ordered into eight linkage groups. The markers included 164 protein-coding genes that were found to fall into several gene-rich clusters with a marker density that would facilitate additional genetic exploitation of this model genus.

MATERIALS AND METHODS

Plant material: We produced an F_2 mapping population ($n = 92$) from a single F_1 progeny of a cross between *A. majus* (as female) and *A. molle* (as male). We had derived the *A. majus* parent, line 165E, by repeated self-pollination of line JI.98, kindly provided by Rosemary Carpenter (JIC, Norwich, United Kingdom). Line JI.98 had itself been produced by >10 generations of self-pollination (Harrison and Carpenter 1979; Sommer *et al.* 1985). We obtained the *A. molle* parent from the IPK (Gatersleben, Germany), from an accession that was probably collected originally in Catalunia, Spain. *A. molle* is entirely self-incompatible and must therefore be maintained by cross-pollination. We found the *A. molle* parent of the mapping population to be heterozygous at many loci and we detected more than two alleles of some loci within the original *A. molle* seed accession. This suggested that repeated sib matings had not been involved in creating the *A. molle* accession and therefore that this mapping parent had experienced little inbreeding. We selected F_2 plants at random and propagated them vegetatively to obtain sufficient leaf tissue for DNA preparation. In addition, we generated two further F_2 populations to examine transmission ratios in hybrids between *A. majus* lines—one by crossing 165E to Sippe 50, a further inbred line of *A. majus,* another by crossing 165E to a morphological mutant with the Sippe 50 genetic background. For each population we genotyped 96 F_2 plants for selected codominant markers.

Molecular analysis: We extracted genomic DNA from frozen young leaves as described by Doyle and Doyle (1987). To detect restriction fragment length polymorphism (RFLP), we digested ~1.5 μg DNA with a panel of restriction enzymes (*Bgl*II, *Eco*RI, *Eco*RV, *Hin*dIII, or *Asn*I), separated it in 1% agarose gels, blotted it onto nylon membranes, and hybridized

it with ^{32}P-labeled probes. Because the *A. molle* parent proved to be heterozygous for polymorphisms at many loci, we detected RFLPs present in the mapping population by comparing the inbred *A. majus* parent with the F_1 hybrid. We assumed that alleles unique to the F_1 had been contributed by *A. molle* and confirmed their origins by linkage analysis. The majority of RFLP markers were detected with expressed sequence tags (ESTs) selected at random from a cDNA library in λ-phage (Sommer *et al.* 1990), subcloned into pUC18, and sequenced (see http://www.antirrhinum.org for details of sequences). Redundancy was eliminated by hybridizing newly isolated inserts with previous probes. Other RFLP markers (shown in the map by the abbreviated gene names) represent the coding or 5′ regions of genes with known mutant phenotypes or their homologs, which were either obtained during our research or kindly provided by Enrico Coen, Cathy Martin, and Des Bradley (JIC, Norwich). In several cases, RFLP probes detected several unlinked polymorphic bands (*e.g.,* 16.1, 16.2, etc.), assumed to represent paralogous loci. We mapped transposon insertion sites (designated *Tam*) as RFLPs using *Tam1, Tam8,* or *Tam9* transposon sequences or flanking sequences as probes.

We mapped 18 loci as codominant cleaved amplified polymorphic sequences (CAPS) and two as dominant markers when primers were able to amplify only one parental allele. We designed primers from the cDNA sequences of *A. majus* genes with known functions or from a collection of *A. majus* ESTs representing ~12,000 unique genes. Other sequences were kindly provided by Jorge Almeida (ITQB, Lisbon) and Cathy Martin and John Doonan (JIC, Norwich). When genomic sequence information was available, we designed primers within exon sequences flanking one or more introns. Where only cDNA sequence was available for *A. majus,* we predicted the positions of introns in conserved coding regions by comparison to Arabidopsis genomic sequences and confirmed the identity of PCR products and the positions of introns by sequencing. We amplified sequences from 6 ng of template DNA and analyzed their digestion products in 1–4% agarose gels.

We produced amplified fragment length polymorphism (AFLP) fragments using the method of Vos *et al.* (1995) with the ^{33}P-labeled *Eco*RI primer E31 and the *Mse*I primers M33, M35, and M36. We separated amplification products in sequencing gels and visualized them by autoradiography.

We amplified inverse sequence tagged repeats (ISTRs), corresponding to *Copia/Ty*-like retroposons, using two ^{33}P-labeled primer combinations as described by Duran *et al.* (1997). We separated products in sequencing gels and detected them by autoradiography (Rohde 1996).

We performed intersimple sequence repeat (ISSR) analysis by PCR amplification from 6 ng DNA template using a single primer [5′-(CA)$_8$T-3′] at the annealing temperature of 50° (Godwin *et al.* 1997) and analyzed products in 1% agarose gels.

Data analysis and linkage mapping: All AFLPs, ISTRs, and ISSRs as well as some RFLP and CAPS markers that detected only one allele were scored for presence/absence. The genotypes of loci with codominant RFLP or CAPS alleles were scored as one of three states (homozygous *A. molle,* homozygous *A. majus,* or heterozygote). Subsequently, these data were transformed into presence/absence values of two segregating alleles. Characteristics of all the markers available for linkage mapping are listed in Table 1.

Deviations from Mendelian segregation ratios of 3:1 for dominant alleles and 1:2:1 for codominant loci were tested using χ^2 values with 1 or 2 d.f., respectively. To represent the threshold for significantly distorted transmission of alleles graphically, the deviation from the expected proportion of

one homozygote (0.25) giving a significant χ^2 value ($\alpha = 0.05$ with 1 d.f.) was calculated as ± 0.16. Fewer codominant loci have allele frequencies outside these thresholds than show significantly distorted transmission overall because calculations of overall transmission ratio distortion were made using all three allelic states. The threshold values therefore can be regarded as conservative for codominant loci.

Linkage analysis, estimation of recombination frequencies, and determination of linear orders between linked loci (including multipoint linkage analysis and the EM algorithm to handle missing data) were performed as described by RITTER et al. (1990) and RITTER and SALAMINI (1996). The MAPRF program (RITTER and SALAMINI 1996) was applied for the computational methods.

The basic procedure consisted of first identifying the allelic configurations (coupling or repulsion) between each pair of markers. Subsequently, χ^2 tests of linkage were performed and recombination frequencies between alleles calculated according to their configuration. Linked markers were arranged into linkage groups using a nearest-neighbor method and a minimum LOD score threshold of 3.0 between at least one pair of markers in the group. The explicit order of markers within linkage groups was determined by obtaining the order that maximized the sum of LOD. Different strategies for constructing linkage maps involving different marker types were applied and compared as described in RESULTS.

Genome length was calculated using method 4 of CHAKRA-VARTI et al. (1991). Map coverage, expressed as the proportion c of a genome within d cM of a marker, was calculated according to FISHMAN et al. (2001).

RESULTS

Identification and mapping of DNA polymorphisms: The two most commonly used laboratory lines of *A. majus* showed a much lower frequency of polymorphisms, detectable as RFLP or CAPS, than *A. majus* compared to other Antirrhinum species. In a prescreen to select appropriate probe-enzyme combinations for RFLP analysis, 70% of probes were found to detect polymorphisms between *A. molle* and *A. majus* for at least one of five restriction enzymes, whereas <20% detected RFLPs within *A. majus* (data not shown). A similar frequency of polymorphisms was detected in CAPS analysis. AFLPs were also about three times more common between *A. majus* and *A. molle* than within *A. majus*. Therefore, to facilitate identification of polymorphic molecular markers, an F_2 mapping population ($n = 92$) was generated from a single F_1 progeny of the interspecific cross *A. majus* $\times$ *A. molle.*

Codominant RFLP or CAPS alleles were detected at 126 loci and dominant alleles at another 38 loci. ISTR and three AFLP primer combinations generated 25 and 99 dominant polymorphic fragments, respectively, and an ISSR primer another four fragments. Comparisons of the alleles in the *A. majus* and F_1 parents, confirmed by testing which alleles were in coupling phase in the F_2, revealed that 80 dominant alleles were descended from *A. molle* and a similar number (86) from *A. majus*. Together with codominant alleles of another 126 loci,

these provided a total of 418 segregating markers at a maximum of 292 different loci (Table 1).

Extensive distortion of allele transmission ratios was observed for all marker types. A total of 161 dominant markers (38.5%) showed significant deviations ($\alpha = 0.05$) from the expected segregation ratio of 3:1 and about half of these (18% of markers) showed deviations that were significant at the higher threshold of $\alpha = 0.005$.

For codominant markers a total of 76 loci (60%) showed significant deviations ($\alpha = 0.05$) from the expected 1:2:1 segregation ratio, and the deviations of more than half of these (31% of loci) were significant at the higher threshold of $\alpha = 0.005$. On average, we found 11.8% fewer homozygotes than expected for *A. molle* alleles and 26.8% fewer for *A. majus* alleles and therefore a genomewide excess of 38.6% heterozygotes. Loci showing distorted transmission ratios mapped throughout the genome, and the nature of distortion also varied with position (see below).

Construction of linkage maps: For the first round of map construction, linkage groups were established using individual alleles of codominant loci and dominant markers linked in coupling phase as described by RITTER et al. (1990). The markers could easily be arranged in 16 linkage groups, corresponding to the parental chromosomes, using a LOD score threshold of 3.0. It was evident which pairs of linkage groups were homologous (in repulsion phase) on the basis of the information available from the integrated codominant markers. However, transmission ratio distortion prevented unambiguous ordering of fragments within linkage groups and the statistically most likely order of markers differed among homologous linkage groups. Therefore, projecting homologous linkage groups onto one linkage group using the method of allelic bridges (RITTER and SALAMINI 1996) was unlikely to be reliable.

In a second approach, codominant and dominant markers were used together. Recombination frequencies (RF) between each pair of markers were calculated using the formulas of RITTER and SALAMINI (1996) to accommodate the different states of codominant and dominant markers. Eight linkage groups could again be established with this method. However, it was not possible to assign an order of loci within these groups consistent with RF values for all pairwise combinations of loci.

A third approach was therefore applied. RF values were calculated only for codominant markers with three allelic states. A minimum LOD score threshold of 3.0 between adjacent markers allowed construction of a core map consisting of 8 linkage groups. The statistically most likely order of markers obtained in this way was also more consistent with RF values for larger intervals. The orders and distances in this core map were therefore fixed and 16 linkage groups, each composed of alleles in coupling phase, were reconstructed from the

TABLE 1

Markers used in map construction

Marker	Type
1	R*
2	R
3	R*
4	R*
6.1	R*
6.2	RO*
8	R
10	R*
11	R*
12	R
13	R*
14.1	RA
14.1	RO*
14.2	RA
14.3	RO
14.5	RA*
15	R
16.1	RA
16.2	RO
16.3	RO*
18	R
19	R*
24	R
25	R*
26.1	R*
26.2	R*
30	R
31	R*
32	R*
33	R
34	R*
37	R*
38	R*
39	R*
40	R
41.1	R
41.2	R*
42	R*
43	R*
45	R*
46	R*
48	R
49	R
52	RA*
55	R*
57	R*
61	R*
63	R*
70	R
74	R*
76	RA*
77	R*
78	R*
81	R*
83	R*
87	R*
88	RA*

(*continued*)

TABLE 1

(Continued)

Marker	Type
89	R
90.1	R
90.2	R
93.1	R*
93.2	R*
103	R*
107	R*
113	R
114	R
118	R
126	R*
131	RO
147	RO
149	R*
153	R*
154	R*
155	R
157	R
158	R*
159.1	RA*
159.2	RA
159.3	RO
165	R*
166	R*
167	R
168	R*
177	R
178	R*
179.1	R
179.2	R*
180	RA
183	R
184	R*
188.1	R
188.2	R
189	R
190	R*
194	RA*
195	R*
200	C
201	C*
202	C*
203	C
204	C
205	C*
206	C*
207	C*
208	C*
209	C
210	C*
211	C
212	CA*
213	CA*
214	P
516.1	R
516.2	R

(*continued*)

TABLE 1

(Continued)

Marker	Type
CDC2C (gi:1321675)	C*
CDC2D (gi:1321677)	C
CENTRORADIALIS (*CEN*)	R
CYCD3B (gi:6448483)	C
CYCLOIDEA (*CYC*)	R*
DEFH11	R
DEFH125 (gi:1816458)	R
DEFH24	R
DEFH49 (gi:1239960)	R
DEFH52	R
DEFH72.1 (gi:1239962)	R
DEFH72.2	R
DEFH84.1	R
DEFH84.2	R
DEFH9.1	A*
DEFH9.2	RA*
DEFH9.3	RO
DEFH9.4	RO*
DEFICIENS (*DEF*)	R*
DELILA (*DEL*)	R
E31/M33	AFLP
E31/M35	AFLP
E31/M36	AFLP
F7B1a	ISTR
F8B4	ISTR
FAP2 (gi:2673869)	P*
FARINELLI (*FAR*)	R*
FIL1 (gi:406308)	R*
FIL2 (gi:441265)	R*
FLORICAULA (*FLO*)	R*
GLOBOSA (*GLO*)	R*
HIRZINA (*HIRZ*)	C
INCOLORATA2 (*INC2*)	R*
INVAGINATA (*INA*)	C*
ISSR814	ISSR
NIVEA (*NIV*)	R
OCTANDRA (*OCT*)	R*
OLIVE (*OLI*)	R*
PALLIDA (*PAL*)	R*
PHANTASTICA (*PHAN*)	CA
PLENA (*PLE*)	R
RADIALIS (*RAD*)	RA*
SBP1 (gi:1183865)	C
SQUAMOSA (*SQUA*)	R*
TAM1	R*
TAM8.1	RA
TAM8.2	RO*
TAM8.3	RO*
Tam8.4	RA
Tam8.5	RA*
Tam9	RO
TAP1 (gi:16066)	R*

Markers showing distorted segregation are indicated with an asterisk. Names for genes with corresponding mutations are shown in full. Genes with known expression patterns and biochemical functions are abbreviated and shown with their database accession numbers. R, RFLP; C, CAPS; P, PCR; O, dominant marker from *A. molle*; A, dominant marker from *A. majus*.

eight groups. All remaining dominant markers were then integrated in coupling phase into the 16 linkage groups. The final linkage map was obtained by projecting each pair of homologous linkage groups onto 1 combined linkage group based on allelic bridges (RITTER and SALAMINI 1996).

Twenty-three markers (14 ISTRs, 6 AFLPs, 1 ISSR, and 1 codominant RFLP marker) showed ambiguous associations to mapped loci. These markers, 7 of which showed severe distortion, were not included.

In 8 cases, AFLP primer combinations revealed pairs of markers in repulsion with RFs of zero, representing potentially codominant alleles of the same locus (see Figure 1). In another 19 cases, markers of the same primer combination were linked in coupling with RF = 0, therefore representing potentially identical loci. These markers are represented in Figure 1 as single loci. Due to this and to the exclusion of ambiguous markers, the minimum estimate for the number of mapped loci was reduced to 243.

The map of eight linkage groups obtained by the third approach described above is displayed in Figure 1 and its characteristics are summarized in Table 2. The total map length (using the Kosambi function; KOSAMBI 1944) was 613 cM with individual linkage groups varying between 33.5 and 96 cM. Each group contained between 15 and 42 markers with an average of 30.4 markers per linkage group. The 243 loci included 118 codominant and 125 dominant markers (Table 2).

The total genome length was estimated to be 658.3 cM. Our map of 613.1 cM would therefore represent ∼93% of the total genome length. Using the methods described by FISHMAN et al. (2001), we estimated 97.5% of the genome to be within 10 cM of a linked marker and 84.2% to be within 5 cM.

Analysis of transmission ratio distortion: Loci showing distorted transmission ratios were widespread (Figure 2). The direction of distortion varied within and between chromosomes. Large parts of LG1, LG3, and LG5 showed an excess of alleles descended from *A. molle*, accompanied mainly by a deficit of homozygotes for *A. majus* alleles, whereas most of LG4 and LG6 showed a reduced frequency of homozygotes for *A. molle* alleles and an excess of *A. majus* alleles. Skewed transmission of alleles in LG7 resulted from reduction in the frequency of both homozygotes relative to heterozygotes. The most severe distortions were observed in the middle of LG1 (lack of *A. majus* homozygotes), at 30 cM on LG4 (absence of *A. molle* homozygotes), and at the lower end of LG6 (absence of *A. molle* homozygotes).

Because the F_2 mapping population consists of interspecific hybrids, one explanation for distorted transmission ratios is that they result from epistatic interaction between alleles derived from different parents. This is expected to result in a lower frequency of plants homozygous for the *A. majus* allele (a) at one locus and for the *A. molle* allele (b) at a second locus. To test for such
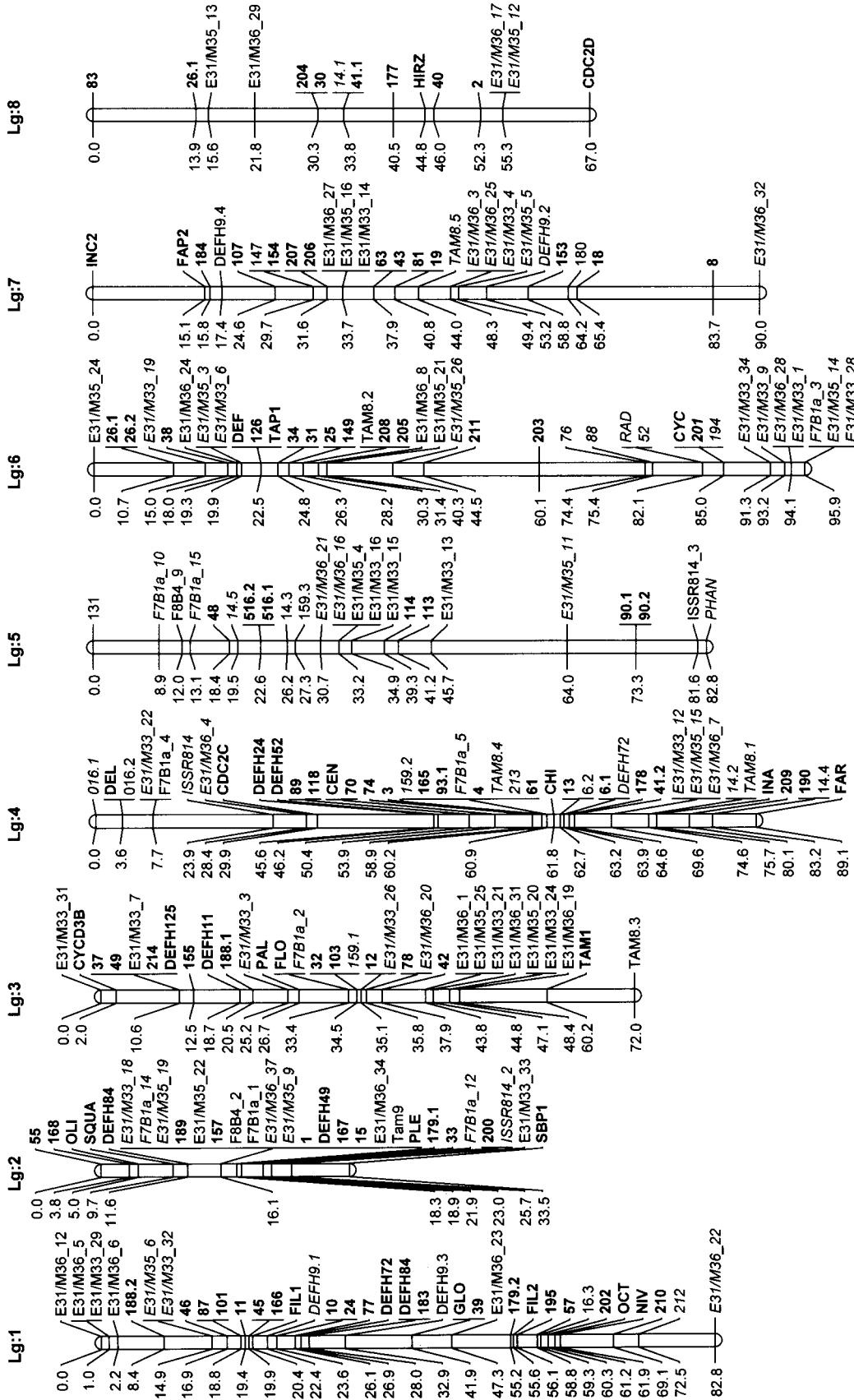
Figure 1.—Linkage map for Antirrhinum derived from an interspecific hybrid between *A. majus* and *A. molle*. Details of markers are listed in Table 1. Distances are given in centimorgans (Kosambi). Loci with codominant markers are in boldface type. Loci represented by dominant alleles from *A. majus* are in italics, while those originating from *A. molle* are in regular type. Loci of noncoding markers that have possible codominant alleles are in boldface italic type.

TABLE 2

Characteristics of the Antirrhinum linkage map

Linkage group	Length (cM)	No. of codominant markers	No. of dominant markers	Total no. of markers
1	82.8	24	12	36
2	33.5	16	13	29
3	72.0	13	18	31
4	89.1	23	19	42
5	82.8	7	16	23
6	95.9	12	28	40
7	90.0	14	13	27
8	67.0	9	6	15
Total	613.1	118	125	243
Mean	76.6	14.8	15.6	30.4

epistatic interactions, regions showing <15% a/a or b/b homozygotes were identified (5 regions from *A. majus* and 10 regions from *A. molle*, including 1 region of LG7 included in both classes). A representative locus with codominant markers, corresponding to the position of maximum distortion, was selected from each region and missing, ambiguous, or anomalous genotypes were replaced by reference to flanking markers. The expected number of a/a b/b homozygotes for each pairwise combination of a/a-depleted and b/b-depleted loci was calculated from the product of the individual homozygous genotype frequencies. The frequency of a/a b/b double homozygotes was significantly lower than expected ($\alpha = 0.05$, using a χ^2 test with 1 d.f.) for only one combination of unlinked loci. The region of LG5 around marker 48 (22% of total length) was underrepresented as *A. majus* homozygotes in plants that were also homozygous for the *A. molle* region of LG8 around marker 26.1 (21% of total length).

A second explanation for distorted transmission ratios is that it results from inbreeding depression and that the reduced frequency of one class of homozygote reflects linkage to a recessive allele that reduces zygote viability in all backgrounds. For example, the lack of plants homozygous for the middle of LG1 from *A. majus* might result from a recessive mutation in this region carried by the *A. majus* parent, 165E. To test this, an F_2 population ($n = 92$) was generated by crossing 165E to a second inbred line of *A. majus*, Sippe 50, and segregation at the *GLOBOSA* (*GLO*) locus in the middle of LG1 analyzed with codominant CAPS markers. As in the interspecific cross, the proportion of plant homozygotes for the *glo* allele from 165E was significantly lower than expected ($\alpha = 0.036$), consistent with the presence of a recessive deleterious allele in this region in line 165E. However, the *CDC2C* locus in the region of LG4 for which *A. molle* homozygotes were not recovered from the interspecific hybrid also showed significantly distorted transmission of alleles from the *A. majus* hybrid ($\alpha =$

0.04), but the direction of distortion was reversed, involving an excess of Sippe 50 homozygotes relative to heterozygotes. Together with the results from LG1, this suggested that transmission ratio distortion is not confined to the interspecific hybrid and that it might have different causes in different hybrid combinations.

For at least one region, the transmission ratio distortion appeared confined to the interspecies cross. The *CYCLOIDEA* (*CYC*) locus of LG6, for which no *A. molle* homozygotes were recovered from the interspecific hybrid, showed undistorted segregation within the *A. majus* hybrid (31 165E homozygotes, 41 heterozygotes, and 24 Sippe 50 homozygotes). This lack of distortion was therefore used in an attempt to compare map distances derived in the presence or absence of distortion. A three-point linkage analysis was made with codominant markers in the region of LG6 around *CYC* using an F_2 population ($n = 96$) segregating 165E and Sippe 50 genetic backgrounds. Map distances calculated from this *A. majus* population were higher than those from the interspecific hybrid—4.17 cM between *CYC* and locus 76 compared to 10.6 cM in the original map and 0.7 cM (a single recombinant) between *CYC* and locus 194 compared to no recombinants in the original population. This suggests that severely distorted transmission might have contributed to an approximately twofold increase in estimated map distances around the *CYC* locus.

DISCUSSION

Various DNA marker types (RFLP, EST, AFLP, ISTR, and ISSR) were successfully applied to detect polymorphisms segregating in the F_2 population of an interspecific hybrid, *A. majus* × *A. molle*. Although significantly distorted transmission ratios were detected for the majority of loci, construction of a robust linkage map was made possible using a framework of codominant markers. This map allowed the potential causes of transmission ratio distortion to be investigated further.

Transmission ratio distortion: Transmission ratio distortion is a characteristic of interspecific hybrids in general (ZAMIR and TADMOR 1986; FISHMAN *et al.* 2001) and has been noted previously for Antirrhinum (HOFFMANN 1949). Theoretically it can result from selection acting at different stages of the life cycle. If selection acts solely on the haploid genotype of F_1 gametophytes or gametes, it should affect the frequency of an allele in F_2 homozygotes and heterozygotes proportionately. If it acts after pollination—due, for example, to a self-incompatibility interaction between haploid pollen grains and diploid maternal tissues or to selection of diploid zygotes—it is likely to affect one of the homozygote classes disproportionately. In the *A. majus* × *A. molle* hybrid, one genotype is usually affected disproportionately, suggesting that selection acts predominantly after pollination or fertilization. This contrasts with other interspecific hybrids
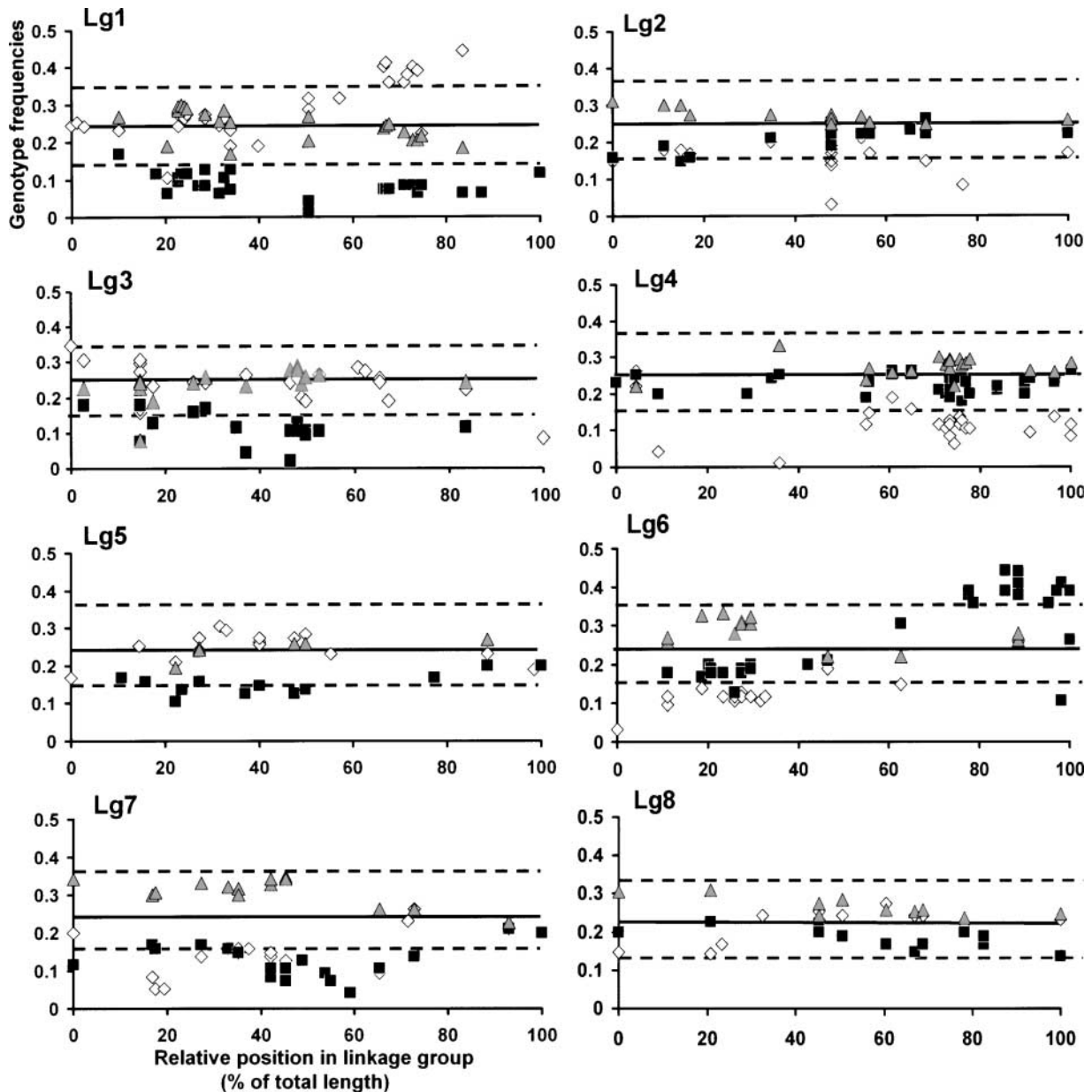
FIGURE 2.—Transmission of parental alleles to the F_2 mapping population. The frequency of *A. majus* homozygotes (solid squares), *A. molle* homozygotes (diamonds), and half the frequency of heterozygotes (shaded triangles) at each locus is plotted against its map position (as a percentage of the linkage group length). All three allelic states are plotted for loci with codominant markers. For loci detected with dominant markers, only the homozygous recessive class is represented. Solid lines represent the frequency (0.25) expected in the absence of transmission ratio distortion and the broken lines represent thresholds for significant distortion of one allelic state compared to the remaining two (95% limits; see MATERIALS AND METHODS).

in which a large component of distortion is likely to reflect selection of haploid gametes or gametophytes (*e.g.*, ZAMIR and TADMOR 1986; KREIKE and STIEKMA 1997).

The proposed selection of genotypes after pollination or fertilization has several potential causes. One explanation is that it represents a case of hybrid breakdown, observed as reduced viability of F_2 progeny (reviewed by JOHNSON 2000). Because hybrid breakdown in plants is often observed first in F_2 progeny, it may involve epistatic interactions between recessive alleles. If this were

the case with the *A. majus* × *A. molle* population, particular combinations of loci homozygous for different parental alleles would be underrepresented. Only one significant association of this type was detected—between loci in LG5 and LG8—and the two loci involved showed only moderate transmission ratio distortion. The relatively small population size is, however, likely to have prevented detection of other epistatic interactions.

A second explanation for distorted transmission ratios is that they result from inbreeding depression and elimination of F_2 zygotes homozygous for deleterious reces-

sive alleles. The population showed an overall deficit of *A. molle* alleles, consistent with the outbreeding *A. molle* carrying more recessive, deleterious mutations than the inbred *A. majus* parent was carrying, as predicted theoretically and observed in other species (*e.g.*, LANDE and SCHEMSKE 1985; CHARLESWORTH and CHARLESWORTH 1987; BAUDRY *et al.* 2001). A reduced frequency of *A. majus* homozygotes was also observed for loci toward the middle of LG1, LG3, and LG7. In the case of LG1, the same *A. majus GLO* allele also showed reduced transmission from a cross to a second *A. majus* line. These results are consistent with the presence of a deleterious allele in LG1 of the *A. majus* mapping parent that disadvantages homozygotes relative to zygotes carrying *A. molle* or different *A. majus* alleles. Similarly, the reduced frequencies of *A. molle* homozygotes toward the top ends of LG4, LG6, and LG7 are consistent with the presence of deleterious *A. molle* alleles in these regions. The relatively small population size prevented more accurate mapping of loci that could account for inbreeding depression (*e.g.*, REMINGTON and O'MALLEY 2000).

An additional explanation for selection against one genotype is that self-incompatibility acts in the F_1 parent to prevent fertilization by pollen grains carrying one parental allele. This is likely to be responsible for the severely distorted transmission of *A. molle* alleles toward the lower end of LG6, including an absence of plants homozygous for *A. molle* alleles of the *CYC* and *RADIALIS* (*RAD*) loci. The self-incompatibility (*S*) locus of several Antirrhinum species is closely linked to *CYC* and *RAD* (BAUR 1919; GRUBER and KÜHL 1932; BRIEGER 1935). The absence of *A. molle* homozygotes suggests that all F_1 pollen carrying the functional *S* allele from *A. molle* are unable to effect self-fertilization and that the eliminated loci are linked to *S* by <1 cM. Consistent with this, we detected no distorted transmission of *CYC* alleles in a hybrid between self-fertile *A. majus* lines. The regions around the *S* loci of other genera are characterized by low recombination frequencies (TANKSLEY *et al.* 1992; LI *et al.* 2000) and therefore association of several markers with the *S* locus of Antirrhinum need not reflect their close physical proximity.

In F_2 hybrids between self-incompatible *A. hispanicum* and self-compatible *A. majus*, one-half of the plants carrying functional *S* alleles from *A. hispanicum* were self-fertile, suggesting that they had inherited a dominant suppressor of self-incompatibility from *A. majus* that was unlinked to *S* (XUE *et al.* 1996). In contrast, we found no F_2 progeny of *A. majus* × *A. molle* that were homozygous for the region around the *A. molle S* allele. One explanation is that suppression is *S* allele specific and that the *A. molle S* allele in our population was not susceptible to suppression in the same way as the allele in the *A. hispanicum* hybrid.

Although self-fertile, *A. majus* has the ability to reject *A. molle* pollen (A. HUDSON and J. F. GOLZ, unpublished results). This phenomenon, an example of unilateral incompatibility, might also contribute to transmission ratio distortion elsewhere in the genome. For example, unilateral incompatibility between *Lycopersicon esculentum* and other Lycopersicon species (members of the Solanaceae, a family closely related to Plantaginaceae) involves interactions between alleles at several loci, including *S* (BERNACCHI and TANKSLEY 1997). Similar interactions in the F_1 of *A. majus* × *A. molle* might therefore cause reduced transmission through pollen of *A. molle* alleles involved in unilateral incompatibility and of *A. majus* incompatibility alleles through ovules.

Many Antirrhinum species, including *A. majus* and *A. molle*, overlap in their geographic ranges and flowering times and are able to form hybrids artificially. However, potential hybrids have been reported only rarely in nature (WEBB 1971; SUTTON 1988). Selection against some hybrid zygote genotypes, as proposed to cause transmission ratio distortion in this experimental mapping population, might have contributed to the scarcity of viable natural hybrids.

Construction of a linkage map: Transmission ratio distortion theoretically can affect map construction in two ways: it can lead to spurious association of distorted loci with loose linkage and it can underestimate distances between closely linked loci (LIU 1998). Algorithms have been developed specifically to deal with the loss of information that results from distortion and affects dominant markers in particular (*e.g.*, LORIEUX *et al.* 1995). Given the significant proportion of codominant markers available for the Antirrhinum population, we tested more general software in a novel approach. Attempts to establish LGs of dominant alleles in coupling phase, treating alleles of codominant loci individually, led to ambiguous alignments. The same was true for LGs constructed with combined dominant and codominant markers. The use of mixed dominant and codominant markers also has the inherent disadvantage of allowing contradictions and unsafe alignments due to the different degrees of accuracy in estimating recombination frequencies (RITTER *et al.* 1990). We therefore adopted the approach of constructing a core map based only on codominant markers and fixing this before adding dominant markers. This allowed use of only one type of estimate, which is also more informative (*i.e.*, has a smaller standard error) than analysis of single alleles in coupling phase (RITTER and SALAMINI 1996).

Limited comparisons of linkage data from the *A. majus* × *A. molle* hybrid and a cross between *A. majus* lines suggest that transmission ratio distortion increased estimates of map distance in the region around the *CYC* locus by about twofold, although suppressed recombination in the interspecific hybrid (discussed below) might partly compensate for the effects of transmission distortion. Further comparative analyses are required to quantify the potential effects of distortion around the *CYC* locus and to determine its effects elsewhere in the Antirrhinum genome. Because the map contained no interval

between markers >20 cM, it is likely that distortion did not lead to spurious fusion of linkage groups during map construction.

We established eight independent linkage groups in our mapping population (*i.e.*, markers at the end of one LG did not show significant linkage to terminal markers of any other LG). These eight LGs may correspond to the eight chromosomes of the haploid Antirrhinum genome. Comparison of the eight linkage groups with the classical map (Stubbe 1966) allows provisional alignment of several linkage groups on the basis of the presence of common markers. LG3 contains the *PALLIDA* (*PAL*) gene and is therefore likely to represent Stubbe's UNI chromosome to which the *pal* mutation maps. Similarly, LG6 corresponds to the *DEFICIENS* (*DEF*) chromosome, LG1 to LUV, LG5 to AUR, on the basis of the presence of the *DEF*, *NIVEA* (*NIV*), and *PHANTASTICA* (*PHAN*) genes, respectively, and LG4 to GRAM, on the basis of the presence of both *DELILA* (*DEL*) and *CENTRORADIALIS* (*CEN*).

Whereas the classical map places *GLO* close to *CEN* on the GRAM chromosome, the molecular map places *GLO* and *CEN* in different linkage groups. Our own experiments have shown independent segregation of *cen* and *glo* mutations in *A. majus*, confirming their unlinked positions in the molecular map. Similarly, *DEF* and *RAD* on LG6 may have been erroneously located on different chromosomes of the classical map. The positions of the few other genes that have been placed in both maps show good agreement: *DEL, NIV, RAD,* and *PHAN* appear near the ends of chromosomes and LGs while *PAL, GLO, DEF,* and *CEN* are located more centrally.

Features and uses of the map: The total length of the Antirrhinum map is ∼610 cM, Kosambi, with an average interval between loci of 2.5 cM (= 610/243). The haploid genome of the *A. majus* parent is estimated to consist of 3.6×10^8 bp (Bennett *et al.* 2000), equating to ∼6×10^5 bp/cM. Markers, particularly those involving protein-coding sequences, showed clustering and clusters occurred both internally and toward the ends of LGs. Similar clustering of coding markers is observed commonly in plant linkage maps. In the case of Antirrhinum it might result from reduced recombination close to centromeres and telomeres, as proposed for other species, including Arabidopsis (*e.g.*, Lister and Dean 1993). It might also partly reflect physical organization of the genome, for example, the nonrandom distribution of noncoding repetitive DNA, as observed at centromeres in six of the Antirrhinum chromosomes (Schmidt and Kudla 1996). AFLP markers, generated from *Eco*RI sites, also occurred in clusters, often outside or between gene-rich regions. Such clustered distribution of AFLP markers is frequently observed in plants and proposed to result from the ability of *Eco*RI to digest methylated DNA associated with noncoding regions (Young *et al.* 1999). Similarly, the majority of retroposon sequences,

detected as ISTRs, mapped outside gene-rich regions and toward the ends of chromosomes, further supporting a model in which genes are physically clustered in the Antirrhinum genome.

Regardless of their origin, the clustering of protein-coding sequences in the map facilitates its use for mapping other genes (as coding sequences, mutations, or quantitative trait loci) because genes have a high probability of being located close to markers in these gene-rich regions. Use of gene-based, codominant markers will also facilitate transfer of these markers to other lines of *A. majus* and to other Antirrhinum species.

The total Antirrhinum map distance is lower than that reported for many plants—*e.g.*, a map of 185 loci of the conifer, *Picea abies*, comprises 3584 cM (Binelli and Bucci 1994). However, the map for Antirrhinum is larger than that obtained for Prunus (491 cM) and similar to that for *A. thaliana* (∼690 cM) with similar numbers of markers (Lister and Dean 1993; Truco *et al.* 1998). Part of the variation in map length is likely to reflect physical differences in genome size: the *P. abies* genome is estimated to be ∼30 times larger than that of *A. majus*, while Prunus and Arabidopsis are estimated to be two and three times smaller, respectively (Bennett and Leitch 1995; Murray 1998; Bennett *et al.* 2000). The disproportionately short length of the Antirrhinum map, when compared, for example, to Arabidopsis, might also reflect reduced recombination frequencies characteristic of interspecific hybrids. For example, the map distances for *Solanum tuberosum* constructed by Kreike and Stiekma (1997) using interspecies hybrids are shorter than that of Gebhardt *et al.* (1991) for two *S. tuberosum* varieties. In the case of Antirrhinum, recombination frequencies between pairs of markers in interspecific hybrids were in general found to be lower than those in crosses between *A. majus* lines (Hoffmann 1949). Reduced recombination may result from small sequence differences between homologous chromosomes, as observed in maize (Dooner and Martínez-Férez 1997). Hemizygous transposon insertions also suppress recombination (Dooner and Martínez-Férez 1997). The *A. majus* parent of the mapping population was selected for high transposon activity (Harrison and Carpenter 1979), and therefore the presence of transposons or of rearrangements generated by transposition might contribute to reduced recombination in its hybrid progeny.

In the *A. majus* × *A. molle* map, 24 different markers mapped to two loci. Seven protein-coding sequences, five AFLPs, and four transposons mapped at 40 cM on LG2, while six genes and two transposons mapped at 61 cM on LG4. Such unusually high densities of markers presumably reflect severely suppressed recombination as the result, for example, of a chromosome inversion. Such inversions can be generated by transposons in *A. majus* (Robbins *et al.* 1989).

Except for LG5 and LG8, all linkage groups contain

one or more of the mapped MADS-box genes, such as *DEF*, *GLO*, *SQUAMOSA* (*SQUA*), *PLENA* (*PLE*), *FARI-NELLI* (*FAR*), and probes designated by "DEFH" (for DEF homologs). This corresponds to the dispersion of members of this transcription-factor gene family observed in other species (FISCHER *et al.* 1995). The observation that a single MADS-box cDNA probe can detect sequences at two different genomic locations presumably reflects a high degree of sequence similarity between recently duplicated family members.

The existence of homologous genes with equivalent mutant phenotypes in Antirrhinum and Arabidopsis allows identification of orthologous sequences and preliminary comparisons of marker orders in the two genera. For instance, the Arabidopsis orthologs of *PAL* (At5g61850) and *FLORICAULA* (*FLO*; At5g4280) within LG3 are linked in Arabidopsis, as are the markers *GLO* and *FIL2* (equivalent to At5g20240 and At5g06860). Similarly, the order of markers 168, *OLIVE*, and 33 within LG2 is the same as that of the respective Arabidopsis genes At5g06870, Atg13630, and At5g35750. The fact, however, that these Arabidopsis genes are all located within chromosome 5 but spread between three different linkage groups (LG1, LG2, and LG3) in Antirrhinum is consistent with extensive chromosomal rearrangements during divergence of the two genera. The extent of synteny in gene orders among Antirrhinum, Arabidopsis, and other model dicots therefore remains to be tested by finer-scale mapping.

LITERATURE CITED

BAUDRY, E., C. KERDELHUÉ, H. INNAN and W. STEPHAN, 2001 Species and recombination effects on DNA variability in the tomato genus. Genetics **58:** 1725–1735.

BAUR, E., 1907 Untersuchungen über die Erblichkeistverhältnisse einer nur in Bastardform lebensfähigen Sippe von *Antirrhinum majus.* Ber. Dtsch. Bot. Gaz. **25:** 442–454.

BAUR, E., 1919 Über Selbsterilität und Kreutzungssterilität in der Gattung *Antirrhinum.* Z. Indukt. Abstammungs Vererbungsl **21:** 48–52.

BENNETT, M. D., and I. J. LEITCH, 1995 Nuclear DNA amounts in angiosperms. Ann. Bot. **76:** 113–176.

BENNETT, M. D., P. BHANDOL and I. J. LEITCH, 2000 Nuclear DNA amounts in angiosperms and their modern uses—807 new estimates. Ann. Bot. **86:** 859–909.

BERNACCHI, D., and S. D. TANKSLEY, 1997 An interspecific backcross of *Lycopersicon esculentum* × *L. hirsutum*: linkage analysis and a QTL study of sexual compatibility factors and floral traits. Genetics **147:** 861–877.

BINELLI, G., and G. BUCCI, 1994 A genetic linkage map of *Picea abies* Karst., based on RAPD markers, as a tool in population genetics. Theor. Appl. Genet. **88:** 283–288.

BONAS, U., H. SOMMER and H. SAEDLER, 1984 The 17-kb Tam-1 element of *Antirrhinum majus* induces a 3 bp duplication upon integration into the chalcone synthase gene. EMBO J. **3:** 1015–1019.

BRIEGER, F. G., 1935 The inheritance of self-sterility and the peloric flower shape in *Antirrhinum.* Genetica **17:** 385–408.

CHAKRAVARTI, A., L. K. LASHER and J. E. REEFER, 1991 A maximum likelihood method for estimating genome length using genetic linkage data. Genetics **128:** 175–182.

CHARLESWORTH, D., and B. CHARLESWORTH, 1987 Inbreeding depression and its evolutionary consequences. Annu. Rev. Ecol. Syst. **18:** 237–268.

COEN, E. S., J. M. ROMERO, S. DOYLE, R. ELIOTT, G. MURPHY and R. CARPENTER, 1990 *floricaula*: a homeotic gene required for flower development in *Antirrhinum majus.* Cell **63:** 1311–1322.

DARWIN, C., 1868 *The Variation of Animals and Plants Under Domestication.* John Murray, London.

DAVIES, B., P. MOTTE, E. KECK, H. SAEDLER, H. SOMMER *et al.*, 1999 PLENA and FARINELLI: redundancy and regulatory interactions between two Antirrhinum MADS-box factors controlling flower development. EMBO J. **18:** 4023–4034.

DOONER, H. K., and I. M. MARTÍNEZ-FÉREZ, 1997 Recombination occurs uniformly within the *bronze* gene, a meiotic recombination hotspot in the maize genome. Plant Cell **9:** 1633–1646.

DOYLE, J. J., and J. L. DOYLE, 1987 A rapid DNA isolation procedure for small quantities of fresh leaf tissue. Phytochem. Bull. **19:** 11–15.

DURAN, Y., W. ROHDE, A. KULLAYA, P. GOIKOETXEA and E. RITTER, 1997 Molecular analysis of East African tall coconut genotypes by DNA marker technology. J. Genet. Breed. **51:** 279–288.

EAST, E. M., 1940 The distribution of self-sterility in the flowering plants. Proc. Am. Phil. Soc. **82:** 449–517.

FISCHER, A., N. BAUM, H. SAEDLER and G. THEISSEN, 1995 Chromosomal mapping of the MADS-box multigene family in *Zea mays.* Nucleic Acids Res. **23:** 1901–1911.

FISHMAN, L., A. J. KELLY, E. MORGAN and J. H. WILLIS, 2001 A genetic map of the *Mimulus guttatus* species complex reveals transmission ratio distortion due to heterospecific interactions. Genetics **159:** 1701–1716.

GEBHARDT, C., E. RITTER, A. BARONE, T. DEBENER, B. WALKEMEIER *et al.*, 1991 RFLP maps of potato and their alignment with the homologous tomato genome. Theor. Appl. Genet. **83:** 49–57.

GODRON, D. A., 1863 Des hybrides vegetaux consíderé au point de vue de leur fécondité ou de la perpétuité ou non-perpétuité de leurs charactères. Ann. Sci. Nat. IV. Série Bot. Trans. **19:** 135–179.

GODWIN, I. D., E. A. B. AITKEN and L. W. SMITH, 1997 Application of inter simple sequence repeat (ISSR) markers to plant genetics. Electrophoresis **18:** 1524–1528.

GOODRICH, J., R. CARPENTER and E. S. COEN, 1992 A common gene regulates pigmentation pattern in diverse plant species. Cell **68:** 955–964.

GRUBER, F., 1932 Über die Verträglichkeitverhältnisse bei einigen selbststerilen Wildsippen von Antirrhinum und über eine selbstfertile Mutante. Zeitschrift für indukt. Abstammungs-u. Vererbungslehre **62:** 429–462.

GRUBER, F., and O. KÜHL, 1932 Untersuchungen über Selbststerilität bei Antirrhinum und über Koppelung der Sterilitätsallele mit dem Faktor für radiäre Blütenform. Z. indukt. Abst.Vererbungsl. **62:** 463–503.

HAMMER, K., S. KNÜPFFER and H. KNÜPFFER, 1990 Das Gaterslebener *Antirrhinum*-sortiment. Kulturpflanze **38:** 91–117.

HARRISON, B. J., and R. CARPENTER, 1979 Resurgence of genetic instability in *Antirrhinum majus.* Mutat. Res. **63:** 47–66.

HERRMANN, V. H., 1973 Selbst-und Kreuzungsinkompatibilität verschiedener *Antirrhinum*-Arten. Biol. Zentralbl. **92:** 773–777.

HOFFMANN, W., 1949 Untersuchungen über Kopplungen bei Antirrhinum. IX. Mitteilung. In einigen Artkreuzungen. Zeitschrift für indukt. Abstammungs-u. Vererbungslehre **83:** 165–202.

JOHNSON, N. A., 2000 Speciation: Dobzhansky-Muller incompatibilities, dominance and gene interactions. Trends Ecol. Evol. **15:** 480–481.

KOSAMBI, D. D., 1944 The estimation of map distances from recombination values. Ann. Eugen. **12:** 172–175.

KREIKE, C. M., and W. J. STIEKMA, 1997 Reduced recombination and distorted segregation in a *Solanum tuberosum* (2×) × *S. pegazzinii* (2×) hybrid. Genome **40:** 180–187.

KÜHL, O., 1937 Genanalyse bei *Antirrhinum*-Artbastarden. Zeitschrift für indukt. Abstammungs-u. Vererbungslehre **74:** 125–160.

KUNZE, R., H. SAEDLER and LÖNNIG, W., 1997 Plant transposable elements. Adv. Bot. Res. **27:** 331–470.

Lande, R., and D. W. Schemske, 1985 The evolution of self-fertilisation and inbreeding depression in plants. 1. Genetic models. Evolution **39:** 24–40.

Li, J. H., N. Nass, M. Kusaba, P. Dodds, N. Treloar *et al.*, 2000 A genetic map of the *Nicotiana alata S* locus that includes three pollen-expressed genes. Theor. Appl. Genet. **100:** 956–964.

Lister, C., and C. Dean, 1993 Recombinant inbred lines for mapping RFLP and phenotypic markers in *Arabidopsis thaliana*. Plant J. **4:** 745–750.

Liu, B.-H., 1998 *Statistical Genomics.* CRC Press, Cleveland/Boca Raton, FL.

Lorieux, M., X. Perrier, B. Goffinet, C. Lanaud and D. G. Deleon, 1995 Segregation distortion. 2. F2 populations. Theor. Appl. Genet. **90:** 81–89.

Luo, D., E. S. Coen, S. Doyle and R. Carpenter, 1991 Pigmentation mutants produced by transposon mutagenesis in *Antirrhinum majus*. Plant J. **1:** 59–69.

Luo, D., R. Carpenter, C. Vincent, L. Copsey and E. Coen, 1996 Origin of floral asymmetry in *Antirrhinum*. Nature **383:** 794–799.

Martin, C. R., R. Carpenter, H. Sommer, H. Saedler and E. S. Coen, 1985 Molecular analysis of instability in flower pigmentation following the isolation of the *pallida* locus by transposon tagging. EMBO. J. **4:** 1625–1630.

Murray, R., 1998 Nuclear DNA amounts in gymnosperms. Ann. Bot. **82** (A): 3–15.

Noda, K., B. J. Glover, P. Linstead and C. Martin, 1994 Flower colour intensity depends on specialized cell shape controlled by a Myb-related transcription factor. Nature **369:** 661–664.

Olmstead, R. G., C. W. de Pamphilis, A. D. Wolfe, N. D. Young, W. J. Elisions *et al.*, 2001 Disintegration of the Scrophulariaceae. Am. J. Bot. **88:** 348–361.

Pohlendt, G., 1942 Cytologische Untersuchungen an Mutanten von *Antirrhinum majus* L. I Deletionen im uni-chromosom. Z. Verebungsl **80:** 281–291.

Remington, D. L., and D. M. O'Malley, 2000 Whole-genome characterization of embryonic stage inbreeding depression in a selfed loblolly pine family. Genetics **155:** 337–348.

Rieger, R., 1957 Inhomologenpaarung und Meioseablauf bei haploiden Formen von *Antirrhinum majus* L. Chromosoma **9:** 1–38.

Ritter, E., and F. Salamini, 1996 The calculation of recombination frequencies in crosses of allogamous plant species with application to linkage mapping. Genet. Res. **67:** 55–65.

Ritter, E., C. Gebhardt and F. Salamini, 1990 Estimation of recombination frequencies and construction of RFLP linkage maps in plants from crosses between heterozygous parents. Genetics **125:** 645–654.

Robbins, T. P., R. Carpenter and E. S. Coen, 1989 A chromosome rearrangement suggests that donor and recipient sites are associated during Tam3 transposition in *Antirrhinum majus*. EMBO J. **8:** 5–13.

Rohde, W., 1996 Inverse sequence-tagged repeat (ISTR) analysis: a novel and universal PCR-based technique for genome analysis in the plant and animal kingdom. J. Genet. Breed. **50:** 249–261.

Schmidt, T., and J. Kudla, 1996 The molecular structure, chromosomal organisation and interspecies distribution of tandemly repeated DNA sequences in *Antirrhinum majus* L. Genome **39:** 248–258.

Soltis, P. S., D. E. Soltis and M. W. Chase, 1999 Angiosperm phylogeny inferred from multiple genes as a tool for comparative biology. Nature **402:** 402–404.

Sommer, H., R. Carpenter, B. J. Harrison and H. Saedler, 1985 The transposable element Tam3 of *Antirrhinum majus* generates a novel type of sequence alterations upon excision. Mol. Gen. Genet. **199:** 225–231.

Sommer, H., J. P. Beltran, P. Huijser, H. Pape, W. E. Lönnig *et al.*, 1990 *Deficiens*, a homeotic gene involved in the control of flower morphogenesis in *Antirrhinum majus*: the protein shows homology to transcription factors. EMBO J. **9:** 605–613.

Stubbe, H., 1966 *Genetik und Zytologie von* Antirrhinum *L. sect. Antirrhinum*. VEB Gustav Fischer Verlag, Jena, Germany.

Sutton, D. A., 1988 *A Revision of the Tribe Antirrhineae.* Oxford University Press, London/New York/Oxford.

Tanksley, S. D., M. W. Ganal, J. P. Prince, M. C. de Vicente, M. W. Bonierbale *et al.*, 1992 High density molecular linkage maps of the tomato and potato genomes. Genetics **132:** 1141–1160.

Truco, M. J., R. Messeguer, I. Batlle, R. Quarta, E. Dirlewanger *et al.*, 1998 Construction of a saturated linkage map for *Prunus* using an almond × peach F2 progeny. Theor. Appl. Genet. **97:** 1034–1041.

Vos, P., R. Hogers, M. Bleeker, M. Reijans, T. Van de Lee *et al.*, 1995 AFLP: a new technique for DNA fingerprinting. Nucleic Acids Res. **23:** 4407–4414.

Waites, R., H. R. N. Selvadurai, I. R. Oliver and A. Hudson, 1998 The *PHANTASTICA* gene encodes a MYB transcription factor involved in growth and dorsiventrality of lateral organs in *Antirrhinum*. Cell **93:** 779–789.

Webb, D. A., 1971 Taxonomic notes on *Antirrhinum*. Bot. J. Linn. Soc. **64:** 271–275.

Wheldale, M., 1907 The inheritance of flower colour in *Antirrhinum majus*. Proc. R. Soc. Lond. Ser. B Biol. Sci. **79:** 288–305.

Xue, Y., R. Carpenter, H. G. Dickinson and E. S. Coen, 1996 Origin of allelic diversity in *Antirrhinum S* locus RNases. Plant Cell **8:** 805–814.

Young, W. P., J. P. Schupp and P. Keim, 1999 DNA methylation and AFLP marker distribution in soybean. Theor. Appl. Genet. **99:** 785–792.

Zamir, D., and Y. Tadmor, 1986 Unequal segregation of nuclear genes in plants. Bot. Gaz. **147:** 355–358.